Acknowledgment. The authors acknowledge the support of this research by the National Science Foundation and the Office of Naval Research.

Registry No. $RhCl(P(4\text{-tolyl})_3)_3$, 24554-70-9; $RhCl(P(4\text{-tolyl})_3)_2Py$, 83984-11-6; $RhCl(P(4\text{-tolyl})_3)_2THTP$, 83999-92-2; $RhCl(P(4\text{-tolyl})_3)_2MeIm$, 83984-12-7; $HzRhCl(P(4\text{-tolyl})_3)_3$, 84025-97-8; $HzRhCl(P(4\text{-tolyl})_3)_2Py$, 83984-13-8; $HzRhCl(P(4\text{-tolyl})_3)_2THTP$, 83984-14-9; $HzRhCl(P(4\text{-tolyl})_3)_2MeIm$, 83984-15-0; $[RhCl(P(4\text{-tolyl})_3)_2]_2$, 53127-35-8.

Supplementary Material Available: Listing of calorimetric data for reaction 3 and thermodynamic data for reaction 4 (5 pages). Ordering information is given on any current masthead page.

Pyridoxamine and 2-Oxalopropionic Acid in Aqueous Systems: Conditional Imine Formation Constants and Rate Constants of Vitamin B_6 Catalyzed Decarboxylation

Gregory Kubala† and Arthur E. Martell*

Contribution from the Department of Chemistry, Texas A&M University, College Station, Texas 77843. *Received May 17, 1982*

Abstract: The conditional Schiff base formation constants (K_c) of pyridoxamine (PM) and 2-oxalopropionic acid (OPA) were determined spectrophotometrically in basic aqueous solutions. These equilibrium constants exhibit pH dependence with maximum ketimine formation occurring near pH 9.0 (K_c = 9.6). The kinetics of the vitamin B_6 catalyzed decarboxylation of OPA have been studied spectrophotometrically, and the observed rate constant of decarboxylation (k_{obsd}) exhibited pH dependence with the maximum occurring at approximately the pH corresponding to maximum ketimine formation ($k_{obsd} = 15.6 \times 10^{-4}$ s^{-1} at 1.01×10^{-4} M OPA and 1.00×10^{-5} M PM). Microscopic rate constants (k_{SB}) for the decarboxylation of the Schiff base species present in solution also showed pH dependence with the greatest catalytic activity at pH 7.0 (k_{SB} = 38.4 s^{-1}) and the least at pH 12.47 (k_{SB} = 0.2 s^{-1}). The relative magnitudes of the k_{SB}'s determined are discussed in terms of the various protonated forms of the OPA:PM ketimine, and the corresponding pK_a's have been estimated from the rate constant-pH profiles.

The kinetic and equilibrium studies of the 2-oxalopropionic acid:pyridoxamine system presented here are part of the series of comprehensive investigations on the decarboxylation of 2-oxalopropionic acid (OPA) to α-ketobutyric acid (AKBA) conducted in this laboratory. Previous kinetic work involved the proton-, aluminum(III)-, copper(II)-, and zinc(II)-catalyzed decarboxylation[1-3] of OPA, and a related study of proton association and metal ion stability constants for each species formed in solution has been reported.[4] Such investigations have been and continue to be of interest because of the importance of β-carboxy-α-ketocarboxylic acids in metabolic reactions in biological systems. Additional investigations reported to date have involved the spontaneous,[5-12] metal ion catalyzed,[8-21] and enzymatic[22] decarboxylation reactions along with the corresponding enolization,[23-25] dehydration,[23,25] and hydration[25] reactions. Additional substrates which have been employed in these studies are oxaloacetic acid (OAA), dimethyloxaloacetic acid (DMOAA), and fluorooxaloacetic acid, which undergo decarboxylation to form pyruvic, α-ketoisovaleric, and fluoropyruvic acids, respectively.

The extensive studies conducted on these substrates provided a nearly complete understanding of the spontaneous and metal ion catalyzed decarboxylation of β-carboxy-α-ketocarboxylic acids. Such knowledge was and still is considered a prerequisite to the interpretation of the vitamin B_6 catalyzed systems which in turn are important for comparison with the corresponding enzyme-catalyzed biological processes. Schiff bases of OAA and its analogues with pyridoxamine are probable intermediates for the decarboxylation of the corresponding aminodicarboxylic acids such as L-aspartic acid and may be formed by transamination of the latter.

The decarboxylation of 2-oxalopropionic acid in the presence of pyridoxamine (PM)[26] has been previously reported, but this study was limited to product analysis and the specification of the reaction conditions employed. In that same investigation, Sakkab

Scheme I

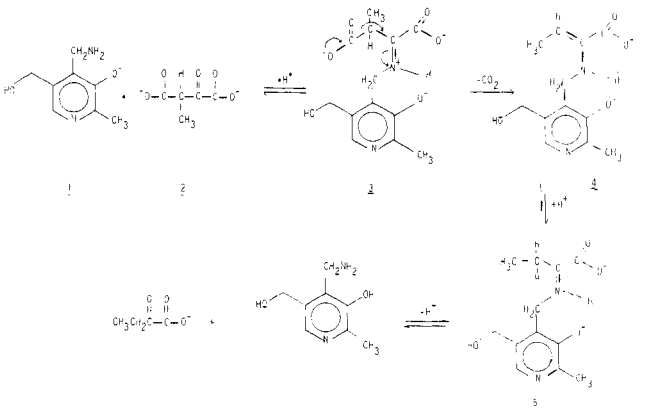

† Abstracted in part from a dissertation submitted by Gregory Kubala to the Faculty of Texas A&M University in partial fulfillment of the requirements for the degree of Doctor of Philosophy.

(1) Kubala, G.; Martell, A. E. *J. Am. Chem. Soc.* **1981**, *103*, 7609.
(2) Kubala, G.; Martell, A. E. *Inorg. Chem.* **1982**, *21*, 3007.
(3) Sakkab, N. Y.; Martell, A. E. *J. Am. Chem. Soc.* **1976**, *98*, 5285.
(4) Kubala, G.; Martell, A. E. *J. Am. Chem. Soc.*, in press.
(5) Ochoa, S. *J. Biol. Chem.* **1948**, *174*, 115.
(6) Gelles, E. *J. Chem. Soc.* **1956**, 4736.
(7) Steinberger, R.; Westheimer, F. H. *J. Am. Chem. Soc.* **1949**, *71*, 4158.
(8) Kornberg, A.; Ochoa, S.; Mehler, A. H. *J. Biol. Chem.* **1948**, *174*, 159.
(9) Krebs, H. A. *Biochem. J.* **1942**, *36*, 303.
(10) Pedersen, K. J. *Acta Chem. Scand.* **1952**, *6*, 285.
(11) Kosicki, G. W.; Lipovac, S. N. *Can. J. Chem.* **1964**, *42*, 403.
(12) Dummel, R. J.; Berry, M. H.; Kun, E. *Mol. Pharmacol.* **1941**, *7*, 367.
(13) Steinberger, R.; Westheimer, F. H. *J. Am. Chem. Soc.* **1951**, *73*, 429.
(14) Nossal, P. M. *Aust. J. Exp. Biol. Med. Sci.* **1949**, *27*, 143, 312.
(15) Gelles, E.; Salama, A. *J. Chem. Soc.* **1958**, 3689.
(16) Speck, J. F. *J. Biol. Chem.* **1949**, *178*, 315.
(17) Munakata, M.; Matsui, M.; Tabushi, M.; Shigemaisu, T. *Bull. Chem. Soc. Jpn.* **1970**, *43*, 114.

0002-7863/83/1505-0449$01.50/0

Table I. Absorbance Data[a] Used in the Calculations of the Conditional Formation Constants for the Pyridoxamine:OPA Schiff Base

pH	λ_{max}, nm	optical density	optical density in the presence of OPA[b] 0.0868 M	0.152 M	0.199 M	0.324 M	buffering agent
7.00	325	0.628	0.601	0.583	0.572	0.547	phosphate
7.52	352	0.629	0.584	0.556	0.540	0.503	triethanolamine
7.98	325	0.598	0.490	0.438	0.410	0.356	triethanolamine
8.45	315	0.551	0.406	0.345	0.314	0.260	triethanolamine
8.78	315	0.550	0.381	0.317	0.285	0.231	*N,N*-dimethylglycine
9.00	310	0.556	0.380	0.315	0.284	0.231	*N,N*-dimethylglycine
9.18	310	0.557	0.382	0.318	0.286	0.233	borate
9.41	310	0.556	0.393	0.330	0.299	0.246	borate
9.83	310	0.556	0.388	0.323	0.290	0.247	carbonate
10.01	310	0.558	0.442	0.394	0.370	0.327	carbonate
10.84	310	0.575	0.503	0.467	0.447	0.409	triethylamine
11.70	307	0.600	0.540	0.509	0.491	0.455	dimethylgyoxime
12.47	307	0.650	0.578	0.561	0.550	0.525	

[a] All solutions 8.602×10^{-4} M pyridoxamine in 0.100 M KCl; 25.0 °C, buffer strength 0.100 M. [b] Extrapolated to time of mixing.

and Martell[26] studied the decarboxylation of L-aspartic acid in the presence of pyridoxal and Al(III) and demonstrated that prior transamination from the aldimine to the ketimine occurs before decarboxylation. Martell and Langohr[27,28] have reported metal ion and pyridoxal-catalyzed dephosphonylation reactions and proposed a mechanism analogous to that considered applicable to β-carboxy-α-ketocarboxylic acids. It is the primary goal of this investigation to study the mechanisms of pyridoxamine-catalyzed reactions of OPA and its analogues (Scheme I) and the initial step involving condensation of the primary amino acid function of pyridoxamine (**1**) with the the carbonyl group of OPA (**2**) to form the ketimine Schiff base intermediate **3**. The decarboxylation reaction is considered to involve the shift of the electron pair between the β- and γ-carbon atoms, resulting in the formation of intermediate **4**. The electron pair thus released becomes localized at the azomethine nitrogen. Subsequent hydrolysis of intermediate **5** is thought to occur with the formation of α-ketobutyric acid and pyridoxamine. It is essential that kinetic and equilibrium data be obtained in order to determine the reaction intermediates and to elucidate the mechanism of the reaction under consideration. This is the first such study reported for a β-carboxy-α-ketocarboxylic acid:pyridoxamine Schiff base system.

Experimental Section

Materials. 2-Oxalopropionic acid was prepared by acid hydrolysis of diethyl oxalopropionate, purchased from Aldrich Chemical Co., according to the procedure described by Kubala and Martell.[1] OPA is hygroscopic and should be handled in a cold room and/or under dry nitrogen whenever possible. OPA solutions were prepared with doubly distilled water, and stock solutions for kinetic runs were stored at 0 °C and brought to 25.0 °C just before each experiment. These stock solutions were discarded 5 h after preparation. The concentration of 2-oxalopropionic acid stock solutions was about 1.00×10^{-3} M and was determined by titration with standardized carbonate free aqueous KOH. The supporting electrolyte was potassium chloride and was obtained as reagent grade material. Pyridoxamine dihydrochloride was purchased from Sigma Chemical Co. and was used without further purification. Stock solutions of PM were prepared at a concentration of 1.00×10^{-3} M, stored in a refrigerator, and discarded after 2 days. The pH of the stock solutions and reaction mixtures was controlled by the addition of aqueous HCl or a carbonate-free solution of KOH prepared from Dilut-it ampules.

Measurements. The pH values were obtained with a Beckman research pH meter fitted with Fisher reference and universal glass electrodes. The meter was standardized so as to read hydrogen ion concentration directly.

Kinetic data were obtained by monitoring the maximum absorption in the ultraviolet region of OPA, which occurs at 260 nm acertain pH values. Pyridoxamine also absorbs light at this wavelength. Since in the kinetic studies the concentration of PM is 1.00×10^{-5} M and that of OPA is 1.00×10^{-4} M and since the Schiff base formation constant between the two is small, it is assumed that both OPA and PM exist as 99.9+% in their free forms. The molar absorptivity of pyridoxamine at 260 nm was measured at various pH values and a simple calculation, described in the computation section of the Experimental Section, was used to correct the magnitude of the observed absorbance measurement to reflect only the optical density of the OPA component in the reaction mixture. The absorbance of PM was calculated and not measured from an infinity spectrum of the reaction system since over longer periods of time transamination occurs and a mixture of pyridoxamine and pyridoxal exists. The absorptivity was measured on a Cary-14 recording spectrophotometer with quartz cells having 5.00-cm path length for the kinetic experiments and 0.100-cm path length for the equilibrium measurements. The absorptivity of the reaction solutions was measured in an experimental set up which allowed simultaneous measurements of ultraviolet absorption spectra and pH. The temperature of the reaction vessel and quartz cells were maintained at 25.00 ± 0.05 °C with a constant temperature bath. The ionic strength of the reaction solutions was maintained at 0.100 M with KCl.

Kinetic measurements were conducted on unbuffered solutions in order to eliminate the catalytic effects which buffers have on the rate of decarboxylation. The absence of buffers allows the accurate calculation of rate constants of decarboxylation of the various Schiff base species in solution. The absence of buffering agents resulted in some drift of the pH in the weakly basic regions during the course of the reaction but error in kinetic values due to this drift was minimized by employing initial rates. The drift was not as large as was first expected, possibly because the system is somewhat selfbuffered. All measurements were taken before the shift in pH became significant. Carbon dioxide is absorbed from the atmosphere above pH 6, but the experimental conditions employed allowed for the collection of accurate data before such absorption became appreciable. The absorptivity of the decarboxylation product, AKBA, was found to be negligible at 260 nm under the present experimental conditions.

Computations. Absorbance extrapolations used in the conditional equilibrium constant determinations were calculated by a linear least-squares program on a 64K Z-80 microprocessor. The rate of disappearance of the optical density at 260 nm was fitted to eq 1, where A_{OPA}

$$\ln A_{OPA} = -k_{obsd}t + \ln A_{0,OPA} \quad (1)$$

is the absorbance of 2-oxalopropionic acid at time t, and $A_{0,OPA}$ is the initial absorbance of OPA. A_{OPA} is an absorbance value which has been mathematically corrected to represent the absorptivity of only OPA at 260 nm, in accordance with eq 2, where A_{obsd} is the observed optical

$$A_{OPA} = A_{obsd} - A_{PM} \quad (2)$$

density and A_{PM} is the calculated absorbance of pyridoxamine in the reaction solution.

Results and Discussion

Pyridoxamine Spectra. The ultraviolet spectra from 200 to 350 nm of 8.602×10^{-4} M pyridoxamine at 25.00 °C in 0.100 M KCl

(18) Bontchev, P. R.; Michaylova, V. *J. Inorg. Nucl. Chem.* **1967**, *29*, 2945.
(19) Covey, W. D.; Leussing, D. L. *J. Am. Chem. Soc.* **1974**, *96*, 3860.
(20) Raghaven, N. V.; Leussing, D. L. *J. Am. Chem. Soc.* **1976**, *98*, 723.
(21) Rund, J. V.; Claus, K. G. *J. Am. Chem. Soc.* **1967**, *89*, 2256.
(22) Krampitz, L. D.; Werkman, C. W. *Biochem. J.* **1974**, *34*, 595.
(23) Emly, M.; Leussing, D. L. *J. Am. Chem. Soc.* **1981**, *103*, 628.
(24) Bruice, P. J.; Bruice, T. C. *J. Am. Chem. Soc.* **1978**, *100*, 4793.
(25) Pogson, E. I.; Wolfe, R. G. *Biochem. Biophys. Res. Commun.* **1972**, *46*, 1048.
(26) Sakkab, N. Y.; Martell, A. E. *Bioinorg. Chem.* **1975**, *5*, 67.
(27) Martell, A. E.; Langohr, M. F. *J. Chem. Soc., Chem. Commun.* **1977**, 342.
(28) Martell, A. E.; Langohr, M. F. *J. Inorg. Nucl. Chem.* **1978**, *40*, 149.

Table II. Conditional Formation Constants[a] for Imines Formed by PM with OPA, Pyruvate, and α-Ketobutyrate (t = 25.0 °C, μ = 0.100 M KCl)

K_c(OPA)		K_c(pyruvate)[d]		K_c(AKBA)[b,e]		pyruvate overall formation constants[c,f]
pH	M^{-1}	pH	M^{-1}	pD	M^{-1}	
7.00	1.1	6.70	1.15	2.9	0.2	
7.52	1.6	7.51	2.20	6.0	1.5	$PMP^{3-} + P^- + H^+ \rightleftharpoons H(PMP{\cdot}P)^{3-}$
7.98	3.7	8.03	4.94	8.0	6.8	$\log \beta_{SB} = 11.65$
8.45	5.2	8.49	6.40	10.0	11.1	
8.78	6.4	9.55	9.1			$H(PMP{\cdot}P)^{3-} \rightleftharpoons H^+ + (PMP{\cdot}P)^{4-}$
9.00	6.9	10.55	8.9			$pK_a = 10.6$
9.18	6.8					
9.41	6.3					$PMP^{3-} + P^- \rightleftharpoons (PMP{\cdot}P)^{4-}$
9.83	6.6					$\log \beta_{SB} = 1.1$
10.12	5.3					
10.84	3.3					
11.70	2.9					
12.47	1.2					

[a] From eq 1. [b] Calculated from a plot of Schiff base concentration vs. -log [H^+] at 30 °C. [c] PMP is pyridoxamine 5'-phosphate; P^- is pyruvate; 25.0 °C, μ = 0.500 M KCl. [d] Reference 35. [e] Reference 36. [f] Reference 37.

solution in a 0.100 cm quartz cell were measured in the pH region 7.00–12.47 in buffered solutions. These measurements have been made previously[29,30] but are considered here in order to ascertain the best wavelength between 300 and 350 nm for monitoring the extent of Schiff base formation. The most accurate equilibrium calculations may be obtained at λ_{max} values where the largest decrease in absorption of PM occurs as a result of Schiff base formation. The optical density at a given wavelength and specified pH are reported in Table I along with the buffering agent used to maintain the hydrogen ion concentration. All of the buffers used had no effect on the absorbance in the wavelength region of interest.

Schiff Base Formation. From the optical density data listed in Table I it is possible to calculate an imine formation constant for the equilibrium

$$PM + OPA \rightleftharpoons \text{imine} \qquad (3)$$

$$K_c = \frac{[\text{imine}]}{[PM][OPA]}$$

Each bracket in the formation constant expression 3 denotes the sum of the concentrations of all possible protonated species. This constant is dependent on the pH since the concentration of each protonated species (imine, PM, and OPA) is pH dependent. As a result, K_c is a conditional formation constant as defined in the above equation.

The conditional formation constants have been determined for Schiff base formation in the pyridoxamine:OPA system over the pH range 7.00–12.47. The addition of increasing concentrations of 2-oxalopropionic acid to a fixed concentration of pyridoxamine results in the formation of increasing amounts of imine, as evidence by the decrease in absorption at 310 nm. The lower pH limit is determined by a lack of significant change in the optical density, ascertained by varying the concentration of OPA, and the upper pH limit is set by interference from a very strong absorption at 290 nm attributed to the enolate form of OPA^{3-} which is observable above pH 12.5. Since the absorptivities of Schiff base and pyridoxamine, and absorbing species in solution at this wavelength, conform to Beer's law, the reciprocal of the total keto acid concentration is directly proportional to the reciprocal of the change in absorption at a given wavelength. A plot of such data gives a straight line in which the negative of the ordinate intercept is the value of the formation constant.[28,31,32]

Plots of $1/[OPA]$ vs. $1/\Delta A$ were made from the change in absorbance at specified wavelengths in Table I at constant pH for solutions of 8.602×10^{-4} M PM at increasing concentrations of OPA up to almost 400-fold that of keto acid. Table I lists the

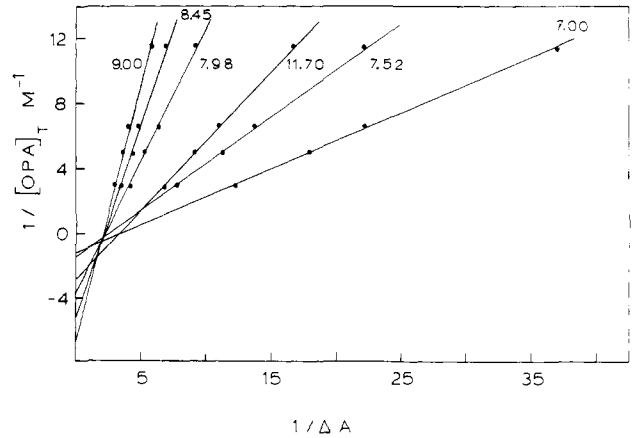

Figure 1. Plots of reciprocal total OPA concentration vs. reciprocal absorbance as a function of pH (-log [H^+]) in 0.100 M KCl solutions at 25.0 °C at 260 nm. Linear plots demonstrate first-order decarboxylation.

absorbance data, pH, and concentrations used in these plots while Figure 1 illustrates representative examples of these plots.

It should be noted at this point that the optical density values employed in the calculation of the conditional formation constants were determined by extrapolating absorbance measurements taken at various times back to the time of mixing. When OPA is allowed to react with pyridoxamine, there is initially a rapid decrease in the absorbance of λ_{max} of pyridoxamine which corresponds to both Schiff base formation between OPA and PM, and decarboxylation to the AKBA:PM imine. After about 20 s, Schiff base formation was assumed to be complete since the rate appeared to be entering the second phase of the observed biphasic change which is attributed solely to the decarboxylation of the OPA:PM imine to the AKBA:imine. A plot of ln OD vs. t is linear for absorbance data in this second phase and extrapolation back to time zero yields the absorbance values listed in Table I. Banks et al.[33] and Felty and Leussing[34] have reported that Schiff base formation between pyruvate and pyridoxamine may take several minutes above pH 9, but equilibrium in the system presently under study usually occurs within 20–30 s. This is reasonable since the additional carboxyl group makes the carbon of the carbonyl more electrophilic, a factor which kinetically facilitates Schiff base formation, but (as will be seen) the second carboxyl thermodynamically destabilizes Schiff base formation.

Figure 2 is a graphical representation of how the conditional equilibrium constants vary with pH and Table II lists the cal-

(29) Matsushima, Y.; Martell, A. E. *J. Am. Chem. Soc.* **1967**, *89*, 1322.
(30) Peterson, E. A.; Sober, H. A. *J. Am. Chem. Soc.* **1954**, *76*, 169.
(31) Lucas, N.; King, N. K.; Brown, S. J. *Biochem. J.* **1962**, *84*, 118.
(32) Oliva, F.; Rossi, C. S.; Siliprandi, N. "Chemical and Biological Aspects of Pyridoxal Catalysis"; Interscience: New York, 1963; p 91.
(33) Banks, B. E. C.; Diamantis, A. A.; Vernon, C. A. *J. Chem. Soc.* **1961**, 4235.
(34) Felty, W. L.; Leussing, D. L. *J. Inorg. Nucl. Chem.* **1974**, *36*, 619.

Scheme II

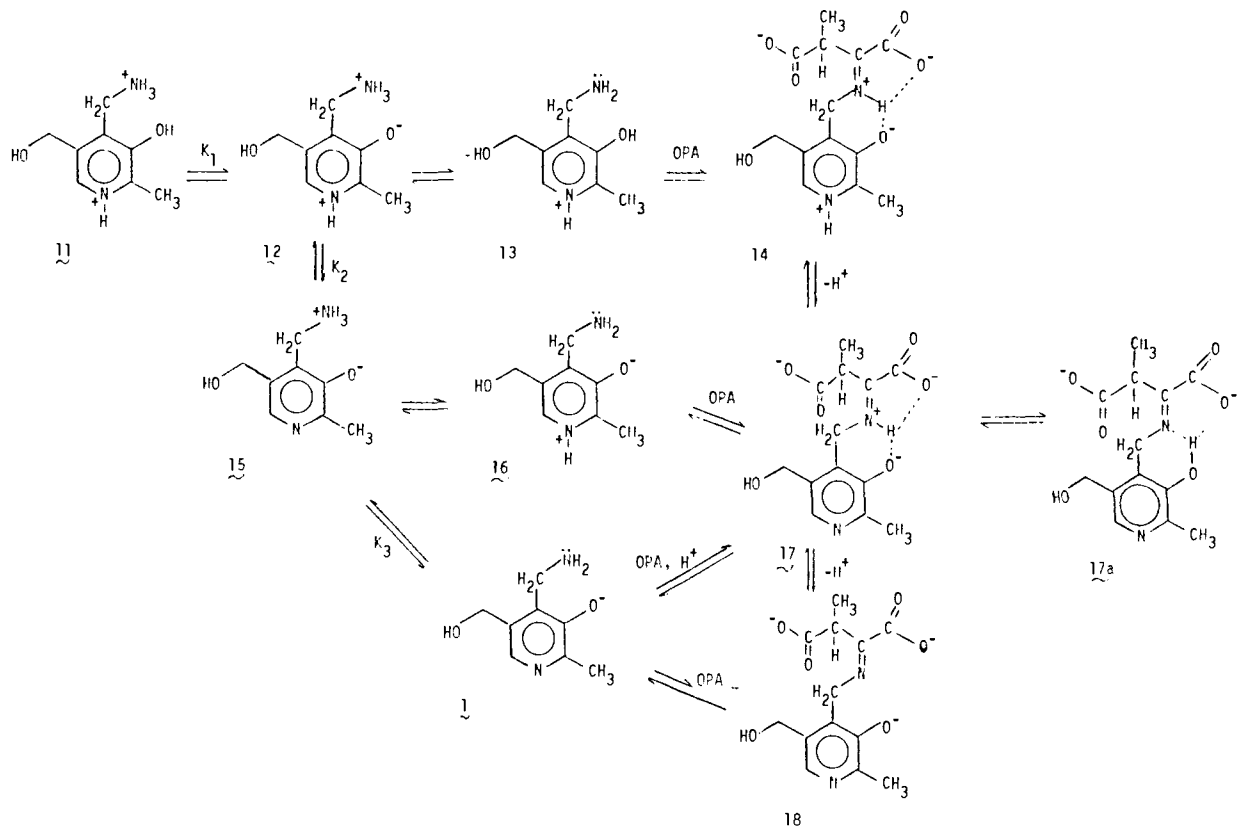

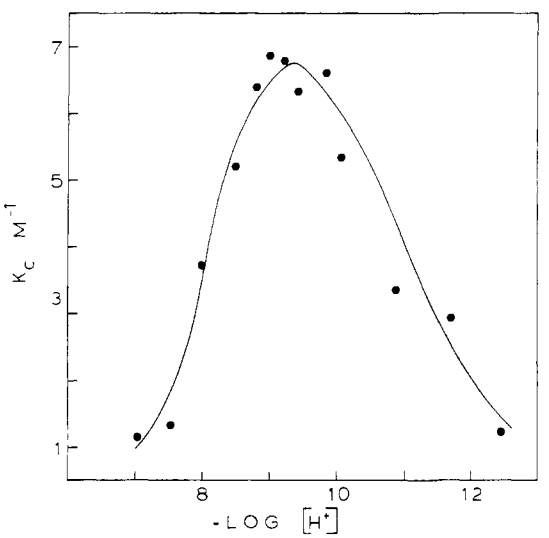

Figure 2. Graphical representation of the dependence on $-\log [H^+]$ of the conditional Schiff base formation constants for OPA and PM.

culated values along with constants of other keto acids for comparison. The general behavior of increasing percent imine from neutral pH to pH 10, and subsequent decrease in Schiff base formation with further increase in hydroxide ion, is similar to the results reported for pyruvate by Felty and Leussing[34] and by Gansow and Holm.[35] Abbott and Martell[36] report similar results for AKBA as have Banks et al.[33] for pyruvate but neither group raised the pH as high as has been done in this study. The pH-dependent behavior may be explained in terms of the various species of OPA and pyridoxamine in solution. The pK_a's of pyridoxamine and 2-oxalopropionic acid have been previously determined and are listed in Table III. The equilibria and species

Table III. Proton Dissociation Constants of 2-Oxalopropionic Acid and Pyridoxamine

compd	pK_1	pK_2	pK_3	ref
OPA	1.75	4.18	13.05	2
PM	3.37	8.01	10.13	38
		8.08	10.3	35
	3.4	8.2	10.2	37

present for OPA have been discussed by Kubala and Martell[2] and are depicted by the formulas. Species **6**, **9**, and **10** are incapable

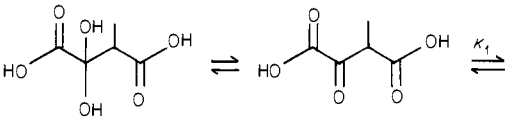

6, Hydrate 7, keto acid

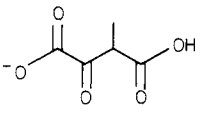

8, keto anion

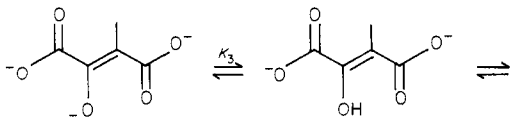

10, enolate 9, enol dianion

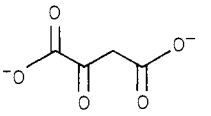

2, keto dianion

of participating in Schiff base formation. The equilibria involved with pyridoxamine solutions are well-known and are included in

(35) Gansow, O. A.; Holm, R. H. *J. Am. Chem. Soc.* **1969**, *91*, 5984.
(36) Abbott, E. H.; Martell, A. E. *J. Am. Chem. Soc.* **1969**, *91*, 6931.

Scheme II. At pH values below 2, Schiff base formation is virtually nonexistent because of the complete protonation of pyridoxamine **11**. Also, a significant amount of OPA is in the hydrate form, **6**, which lacks the carbonyl function. The lone electron pair on the amino nitrogen and the free carbon group are necessary for imine formation, and their protonation and hydration reactions reduce the tendency toward Schiff base formation. For these reasons, appreciable Schiff base formation is not expected at low pH, a conclusion that is supported by Sakkab and Martell[3] who reported that pyridoxamine catalysis of OPA decarboxylation at pD ~2 was not observed.

Between pH 4 and 7, the predominant form of pyridoxamine is species **12** (Scheme II) which is not expected to undergo imine formation. However, **12** is in equilibrium with a minor species **13**, which is capable of forming a Schiff base with the keto dianion **2**, the predominant form of OPA in this pH region, resulting in the formation of imine **14**. As the pH is increased above 7, the predominant form of pyridoxamine is **15** which is in equilibrium with minor species **16**. The predominant OPA form in this region of hydrogen ion concentration is still the keto dianion **2**, and the resulting Schiff base is 17. As the pH is further increased above 9, the major form of pyridoxamine, **1**, quite readily forms Schiff base with OPA to form **17**, which is stabilized somewhat by protonation. Above pH 11 the Schiff base dissociates to form **18**. Without the protonated azomethine nitrogen the Schiff base is relatively unstable and highly susceptible to base-catalyzed hydrolysis, resulting in a decrease of Schiff base formation.

The interpretation presented obove is consistent with the pH-dependent behavior observed for the conditional formation constant, K_C, and is analogou to the pyruvate:vitamin B_6[33-35,37] and AKBA:pyridoxamine[36] systems mentioned earlier. In Table II it is seen that the conditional formation constant of OPA is smaller than those of the keto monocarboxylic acid analogues at a given pH. This is reasonable since the OPA keto dianion is involved in a competing equilibrium with the enol dianion, **9**, which is incapable of undergoing imine formation. The additional equilibrium reduces the amount of keto dianion **4** present and therefore reduces the extent of Schiff base formation. At pH values greater than 12, the conditional formation constant is expected to be even smaller relative to that of the monocarboxylic keto acids since the negative enolate species, **10**, becomes significant at high pH, resulting in further decrease in the concentration of the keto dianion **2**. Also, at high pH OPA may undergo aldol condensation, a reaction which would further reduce the concentration of keto dianion.

Vitamin B_6 Catalysis. Since the systems employed for kinetic runs were dilute and the conditional formation constants are small, only a very small percentage (<0.1%) of the total amount of 2-oxalopropionic acid exists as Schiff base. It is assumed that equilibrium is achieved rapidly in these systems for reasons discussed previously. A second benefit of carrying on kinetic experiments on these dilute systems is that enhancement of the rate of decarboxylation resulting from Schiff base formation is small but measurable. Such considerations are important since equilibrium between the keto dianion of OPA and the dianion of the enol form must be maintained. The reduction of the OPA absorbance at 260 nm reflects the change in concentration of the enol species and can only be directly related to the overall OPA concentration if equilibrium is maintained throughout the reaction being studied.

Kinetic data were obtained by monitoring the decrease in optical density at 260 nm. The absorbing species are pyridoxamine and enolic OPA, **9**, and at this wavelength in alkaline solution the molar absorptivity of PM is much larger than that of 2-oxalopropionic acid. As a result it was necessary to employ a 10-fold molar excess of substrate over pyridoxamine. Under these conditions the major fraction of the optical density is OPA dependent, resulting in a significant change in absorbance as decarboxylation occurs. The total absorbance measured at a given time and pH was corrected to correspond to OPA absorbance by eq 2 as explained in the Experimental Section. The values thus obtained are listed in Table IV. These absorbance values conform to a first-order decomposition rate law and were treated according to eq 1 with the use of a linear least-squares program. The observed decarboxylation rate constants (k_{obsd} calculated in this manner are listed in Table IV and Figure 3 shows several representative plots of $-\ln A_{OPA}$ vs. time. The values of k_{obsd} are also presented graphically in Figure 4 as a pH–rate profile. It is seen that the observed rate constants of catalytic decarboxylation increase above pH 7 until a maximum is reached at pH 9, above which they rapidly decrease in magnitude. Comparison of Figure 4 with Figure 2 demonstrates that enhancement in decarboxylation is directly related to the extent of Schiff base formation.

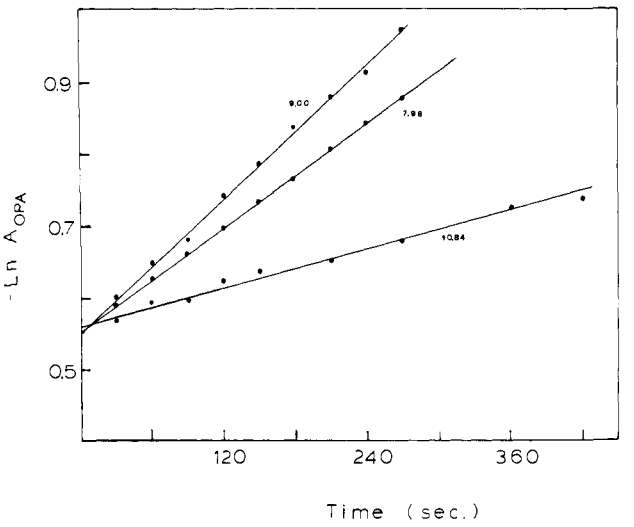

Figure 3. Graphs showing first-order behavior for the decrease in absorbance at 260 nm attributed to the decarboxylation of OPA in the presence of PM. Concentrations of OPA and PM were 1.01×10^{-4} M and 1.00×10^{-5}M, respectively, in 0.100 M aqueous KCl at 25 °C.

Under any given set of experimental conditions, the observed rate constant of decarboxylation may be expressed as the sum of the specific rate constants for OPA and its Schiff base, as indicated in eq 4 where α_{OPA} is the fraction of total OPA in the dianion form, α_{SB} is the remaining portion of OPA which is present as the Schiff base, and k_{OPA} and k_{SB} are the respective first-order rate constants for the individual species. The value of k_{OPA} has previously been determined by Kubala and Martell[1] as 7.75×10^{-5} s^{-1}, and its use as a correction factor for catalytic systems containing pyridoxamine has been described.[4] The values of α_{OPA} and α_{SB} may be calculated from eq 3 at specific pH values if the conditional imine formation constant is known. Equation 4 can be rearranged to yield the following expression.

$$k_{obsd} = k_{OPA}\alpha_{OPA} + k_{SB}\alpha_{SB} \quad (4)$$

$$k_{SB} = \frac{(k_{obsd} - k_{OPA}\alpha_{OPA})}{\alpha_{SB}} \quad (5)$$

Values of k_{SB} calculated in this manner are listed in Table IV and are illustrated in Figure 4. The catalytic effects represented by k_{SB} are dependent on two factors: (1) the extent of Schiff base formation and (2) the nature of the pH-dependent Schiff base forms present. The values of k_{SB} determined with eq 5 reflect rate enhancements corresponding only to the second factor—the change in degree of protonation of the Schiff base. Figure 4 shows k_{SB} to have a value of 38.4 s^{-1} at pH 7 and that it rapidly decreases as the pH is increased to 8.5, above which the rate constant remains relatively unchanged up to pH 10. Above pH 10 values of the rate constant once again rapidly decrease with increasing pH. This behavior may be interpreted in terms of Scheme III. The major form of the ketimine present in solution is **14**. The protonated azomethine and pyridine nitrogens provide the driving

(37) Gansow, O. A.; Holm, R. H. *Tetrahedron* **1967**, *24*, 4477.
(38) Gustafson, R. L.; Martell, A. E. *Arch. Biochem. Biophys.* **1957**, *68*, 485.

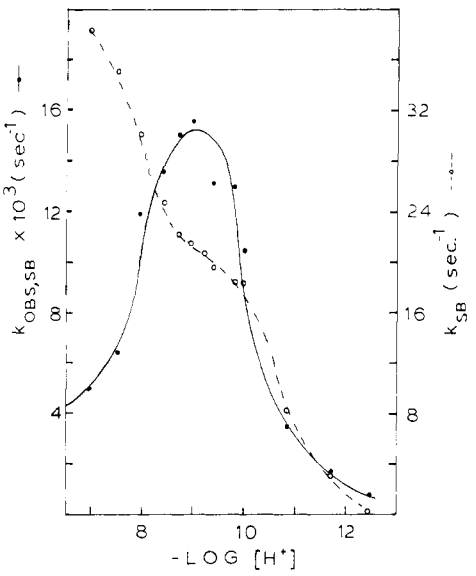

Figure 4. Rate constant profile for the observed ($k_{obsd,SB}$) and Schiff base (k_{SB}) rate constants of OPA decarboxylation as a function of −log [H$^+$]; (-O-) and (−●−) denote the k_{SB} and $k_{obsd,SB}$ plots, respectively.

Scheme III

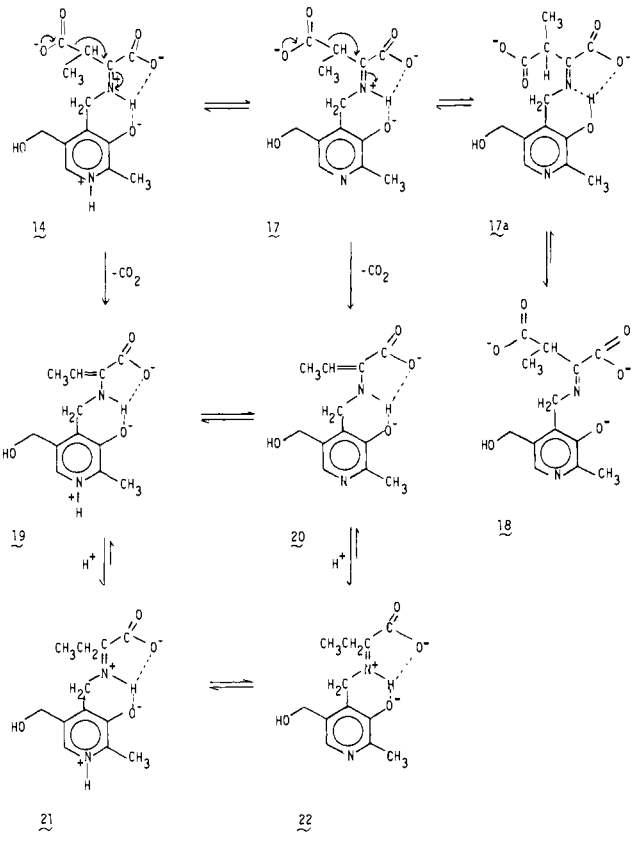

force for the electron shift required for β decarboxylation, since these positively charged groups act as electron sinks.

As the pH is increased to 8.5, deprotonation of the pyridine ring occurs, and the major species present in solution is **17**. In this form the azomethine nitrogen is protonated, but the Schiff base is not as catalytically active toward decarboxylation because of the deprotonation of the pyridine nitrogen. The absence of the positive charge on the pyridine nitrogen results in less stabilization of the negative charge on the phenolic oxygen, thus inducing stronger hydrogen bonding to the hydrogen atom covalently bound to the azomethine nitrogen. This modified hydrogen bond in turn weakens the covalent nature of the N−H bond and slightly decreases the effective positive charge on the azomethine nitrogen,

Table IV. Observed Decarboxylation Rate Constants and Specific Schiff Base Rate Constants with Absorbance Values Employed in Their Calculation[a]

pH	k_{obsd}, 10^4 s^{-1}	variance[b]	k_{SB}, s^{-1}	absorbance (A_{OPA})[c] at specified times, s																	
				30	60	90	120	150	180	210	240	270	330	360	390	420	450	480	510	570	690	720	930	1170
12.47	0.8	0.1	0.2	0.573					0.566				0.558					0.551				0.540	0.531	0.521
11.70	1.7	0.1	3.2	0.571				0.560				0.548		0.540				0.529		0.521	0.510			
10.84	3.5	3.0	8.3	0.566		0.551	0.535	0.528		0.521		0.506		0.485		0.479				0.472				
10.02	10.5	0.2	18.3	0.557		0.523		0.491		0.461		0.433	0.407		0.382	0.370								
9.83	13.0	0.3	18.5	0.552	0.530	0.516	0.490	0.470	0.452	0.434	0.417	0.408												
9.41	13.1	0.3	19.6	0.552	0.530	0.509	0.488	0.469	0.450	0.433	0.415	0.406												
9.18	14.9	0.6	20.8	0.549	0.525	0.509	0.480	0.459	0.439	0.419	0.408	0.383												
9.00	15.6	0.6	21.5	0.548	0.523	0.506	0.476	0.454	0.433	0.413	0.401	0.376												
8.78	15.0	0.9	22.2	0.549	0.523	0.507	0.478	0.457	0.436	0.417	0.408	0.380												
8.45	13.6	0.6	24.7	0.551	0.529	0.514	0.486	0.467	0.448	0.429	0.412	0.403												
7.98	11.9	0.1	30.1	0.554	0.534	0.516	0.498	0.480	0.463	0.447	0.431	0.416												
7.52	5.4	0.1	35.1	0.563		0.542		0.522		0.502		0.483	0.465		0.488		0.431		0.415					
7.00	5.0	0.1	38.4	0.566		0.549		0.533		0.517		0.502	0.488		0.473		0.459		0.446					

[a] 1.01×10^{-4} M OPA and 1.00×10^{-5} M PPM, 25.00 °C, $\mu = 0.100$ M KCl. [b] Variance in slope determined by linear least-squares program. [c] At 260 nm with 5.00-cm path length quartz cells.

thus accounting for some reduction in the catalysis of decarboxylation. An additional pathway for the inductive effect of the pyridine nitrogen involves the α'-carbon directly. The inductive effect of the pyridine nitrogen is partially distributed around the aromatic ring, so that the azomethine nitrogen is separated from this effect by only a single aliphatic carbon atom. It has been suggested by a reviewer of this paper that deprotonation of the pyridine nitrogen may favor a shift of the azomethine proton to the phenolate oxygen resulting in the formation of a new microspecies, **17a**. This change in bonding would have a considerable influence on the rates, over a wide range of **17** $\rightleftharpoons$ **17a** equilibrium quotient. In other words even a small contribution from **17a** would have a pronounced effect.

As the pH is increased above **11**, the major ketimine initially present is **18**. In this species the azomethine nitrogen is now deprotonated, thus accounting for the observed large decrease in catalytic activity. Species **19** and **20** ketonize rapidly to **21** and **22** and dissociate almost quantitatively into AKBA and pyridoxamine since the Schiff base formation constant is small, as are the concentrations of AKBA and PM. α-Ketobutyric acid was identified as the product by NMR measurement on more concentrated solutions and this product was verified earlier by Sakkab and Martell.[32]

It should be possible to estimate the pK_a's of the OPA:pyridoxamine Schiff bases involved in decarboxylation from the inflection points in the pH-rate constant profile of k_{SB} in Figure 4. Not enough data have been collected below the first inflection and beyond the second inflection, for reasons previously mentioned, to carry out a precise determination of the dissociation constants of the Schiff base. However, an estimate of the K_a's defined by eq 6 and 7 observed inflection regions in Figure 4. Thus, the

$$K_{a_1} = \frac{[\mathbf{17}][H^+]}{[\mathbf{14}]} \quad (6)$$

$$K_{a_2} = \frac{[\mathbf{18}][H^+]}{[\mathbf{17}]} \quad (7)$$

mathematical expression for pyridoxamine catalysis over the entire pH range is

$$k_{SB} = k_{H_2A}\alpha_{H_2A} + k_{HA}\alpha_{HA} + k_A\alpha_A \quad (8)$$

with H_2A, HA, and A representing species **14**, **17**, and **18**, respectively. The fraction of each species and the specific rate constant of decarboxylation for each species are α_i and k_i, respectively. Banks et al.[33] have reported 6.9 and 10.3 for the analogous pK_a's in the pyridoxamine:pyruvate ketimine Schiff base system. The specific rate constants indicated in eq 8 were found to be 41.6 s^{-1}, 19.2 s^{-1}, and 0.3 s^{-1} for species **14**, **17**, and **18**, respectively, with an error of ± 0.6 s^{-1}.

The catalytic effects on OPA decarboxylation by pyridoxamine are dependent on two factors: (1) the extent of Schiff base formation and (2) the protonation of the Schiff base species present. On the basis of the specific rate constants determined above, it is proposed that the fully protonated Schiff base is more active toward decarboxylation than the monoprotonated species while the fully deprotonated species is relatively inactive.

Registry No. **1**, 85-87-0; **2**, 642-93-3; **3**, 84065-57-6; vitamin B_6, 8059-24-3.

Nitrosoalkane Complexes of Iron-Porphyrins: Analogy between the Bonding Properties of Nitrosoalkanes and Dioxygen

Daniel Mansuy,*† Pierrette Battioni,† Jean-Claude Chottard,† Claude Riche,‡ and Angèle Chiaroni‡

Contribution from the Laboratoire de Chimie de l'Ecole Normale Supérieure, associé au CNRS, 24 rue Lhomond, 75231 Paris Cedex 05, France, and the Institut de Chimie des Substances Naturelles, CNRS, 91190, Gif-sur-Yvette, France. *Received April 7, 1982*

Abstract: Various iron-porphyrin complexes involving an iron-nitrosoalkane bond, Fe^{II}(porphyrin)(RNO)(L), with porphyrin = TPP, TpClPP, TTP, or DPDME, R = *i*-Pr or Me, and L = MeOH, *i*-PrNHOH, *i*-$PrNH_2$, pyridine, *N*-methylimidazole, or $PPhMe_2$,[1] have been prepared either by reaction of Fe^{II}(porphyrin) with the RNO dimer or of Fe^{III}(porphyrin)(Cl) with RNHOH, in the presence of the L ligand. These hexacoordinate complexes and the pentacoordinate Fe(porphyrin)(RNO) complexes are in the low-spin state and exhibit IR ν_{NO} frequencies ranging from 1400 to 1445 cm^{-1}. Their trans ligands L are in fast exchange, vs. the ^1H NMR time scale, at 20 °C, and bind to the pentacoordinate complex Fe(porphyrin)(RNO) with rather high affinities (for porphyrin = TPP and R = *i*-Pr, the binding equilibrium constants are respectively 350, 6×10^4, and 15×10^4 L mol^{-1} for L = MeOH, pyridine, and *N*-methylimidazole at 27 °C). The X-ray structure of Fe(TPP)(*i*-PrNO)(*i*-$PrNH_2$) shows that *i*-PrNO is bound to the iron by its nitrogen atom, the Fe-N(O)*i*-Pr distance (1.865 (14) Å) being considerably shorter than the Fe-NH_2*i*-Pr distance (2.100 (14) Å). The Fe-N(O)R bond is much stronger than the Fe-N bonds formed with usual amino ligands of iron-porphyrins such as amines, pyridines, or imidazoles. A comparison of some structural, IR, resonance Raman, and Mössbauer data of the Fe(TPP)(*i*-PrNO)(*N*-methylimidazole) and Fe("picket fence"-TPP)(O_2)(*N*-methylimidazole) complexes indicates a great similarity in the bonding properties of the *i*-PrNO and O_2 ligands. These results explain various aspects concerning the formation and properties of hemoglobin- or cytochrome P-450-nitrosoalkane complexes.

There is a considerable current interest in the structural and chemical properties of hemoprotein-iron(II) complexes and in particular in the dioxygen complexes which are the key intermediates in various hemoprotein-dependent enzymatic systems.[2] Recently, evidence has been obtained in favor of the formation of nitrosoalkane complexes of hemoglobin, myoglobin,[3] and cytochrome P-450.[4] In fact, nitrosoalkanes constitute a new class of ligands exhibiting a very high affinity for hemoprotein-iron(II).[5]

† Laboratoire de Chimie de l'Ecole Normale Supérieure.
‡ Institut de Chimie des Substances Naturelles.

(1) Abbreviations: TPP, *meso*-tetraphenylporphyrinate; TpClPP, *meso*-tetra(4-chlorophenyl)porphyrinate; TTP, *meso*-tetratolylporphyrinate; DPDME, deuteroporphyrinate dimethyl ester; P, porphyrinate; *i*-$PrNH_2$, 2-aminopropane; *i*-PrNHOH, 2-(hydroxyamino)propane; *i*-PrNO, 2-nitrosopropane; py, pyridine; *N*-MeIm, *N*-methylimidazole; $PPhMe_2$, dimethylphenylphosphine; Me, methyl; Pyr, pyrrole; Ph, phenyl; MeOH, methanol; s, singulet; d, doublet; t, triplet; h, heptuplet.

0002-7863/83/1505-0455$01.50/0